Available online at www.sciencedirect.com
SCIENCE DIRECT®
International Journal of Heat and Mass Transfer 48 (2005) 4995–5016
International Journal of HEAT and MASS TRANSFER
www.elsevier.com/locate/ijhmt

Film cooling characteristics of rows of round holes at various streamwise angles in a crossflow: Part I. Effectiveness

C.H.N. Yuen, R.F. Martinez-Botas *

Department of Mechanical Engineering, Imperial College of Science, Technology and Medicine, London SW7 2AZ, UK

Received 1 January 2003; received in revised form 12 July 2003
Available online 10 August 2005

Abstract

Film cooling effectiveness were studied experimentally on rows of cylindrical holes with streamwise angles of 30°, 60° and 90°, in a flat plate test facility with a zero pressure gradient. Detailed effectiveness and heat transfer results for a single cylindrical hole at the same inclinations have been presented in Yuen and Martinez-Botas [C.H.N. Yuen, R.F. Martinez-Botas, Film cooling characteristics of a single hole at various streamwise angles: Part I. Effectiveness, Int. J. Heat Mass Transfer 46 (2003) 221–235; C.H.N. Yuen, R.F. Martinez-Botas, Film cooling characteristics of a single hole at various streamwise angles: Part II. Heat transfer coefficient, Int. J. Heat Mass Transfer 46 (2003) 237–249] with the same test facility and measurement technique. This present investigation commenced with a single row of holes with two pitch-to-diameter ratios (p/D) of 3 and 6. It then presents and discusses the effects of introducing inline and staggered rows for each streamwise angle and pitch-to-diameter ratio. The row spacing in the inline and staggered rows is 12.5 diameters in the streamwise direction. The short but engine representative hole length ($L/D = 4$) is constant for all geometries. The blowing ratio ranges from 0.33 to 2, and the freestream Reynolds number based on the freestream velocity and hole diameter (Re_D) was 8563. Both local values and laterally averaged ones are presented, the latter refers to the averaged value across the central hole. The current results are compared with the experimental results obtained by other researchers, the effects of the additional inline and staggered rows, and of the variations in injection angle, pitch-to-diameter ratio are described.

The objectives of the present study are to provide a consistent set of measurements in terms of effectiveness and heat transfer coefficients presented in the companion paper [C.H.N. Yuen, R.F. Martinez-Botas, Film cooling characteristics of rows of round holes at various streamwise angles: Part II. Heat transfer coefficient, Int. J. Heat Mass Transfer, in press], obtained systematically with the same test facility, and to deliver a better understanding of film cooling performance. The present results also serve as a database with 105 test cases, in addition to the 21 cases presented in [C.H.N. Yuen, R.F. Martinez-Botas, Film cooling characteristics of a single hole at various streamwise angles: Part I. Effectiveness, Int. J. Heat Mass Transfer 46 (2003) 221–235], for future numerical modelling.

* Corresponding author. Tel.: +44 20 75947241; fax: +44 20 78238845.
E-mail address: r.botas@ic.ac.uk (R.F. Martinez-Botas).

0017-9310/$ - see front matter © 2005 Elsevier Ltd. All rights reserved.
doi:10.1016/j.ijheatmasstransfer.2005.05.019

Nomenclature

D	hole diameter, 10 mm
HSI	hue, saturation, intensity
L	hole length
M	blowing ratio ($\rho_2 U_2/\rho_\infty U_\infty$)
p	hole pitch or spacing
Re_D	Reynolds number ($\rho_\infty U_\infty D/\mu_\infty$)
RGB	red, green and blue
s	row spacing
SWG	standard gage
T	temperature (K)
U	velocity (m/s)
x	coordinate: streamwise (axial) direction (see Figs. 1 and 2)
y	coordinate: vertical (height-wise) direction (see Fig. 2)
z	coordinate: lateral direction (see Fig. 1)

Greek symbols

δ	boundary layer thickness
δ^*	displacement thickness $\delta^* = \int_0^\delta (1 - \frac{U}{U_\infty})\,dy$
δ_i	momentum thickness $\delta_i = \int_0^\delta (1 - \frac{U}{U_\infty})\frac{U}{U_\infty}\,dy$
η	film cooling effectiveness $\eta = (T_{aw} - T_\infty)/(T_2 - T_\infty)$
ρ	density (kg/m^3)

Subscripts

∞	freestream
2	coolant or secondary injection
aw	adiabatic wall
Overbar	laterally averaged

1. Introduction

The desire for higher specific thrust in air, land and sea gas turbines renders the need for high temperature-rise combustors, and this, in turn, implies increases in turbine entry temperatures. The turbine blades cannot withstand these temperatures and film cooling is required to ensure the required life and usually takes the form of rows of discrete holes along the span of the blades. A major requirement is to ensure that the combustor and blades survive for long periods and with minimum use of cooling air.

The definition of film cooling effectiveness η is given in the nomenclature section. This effectiveness represents the efficiency of a cooling film; the maximum value of unity is achieved when the adiabatic wall temperature is the same as the coolant temperature.

Effectiveness measurements downstream of a row of jets were reported by researchers such as Eriksen and Goldstein [4]; Goldstein and Yoshida [5]; Goldstein et al. [6]; Jabbari and Goldstein [7]; Pedersen et al. [8]; Bergeles [9]; Brown and Saluja [10]; Sinha et al. [11]; Han and Mehendale [12], Vedula and Metzger [13] and Ekkad and Han [14]. From the cited references above, it was suggested for a row of jets of a given streamwise inclination, that effectiveness near the holes increased with increasing blowing ratio, until a certain value beyond which the jets started to lift off, and the effectiveness decreased, and this ratio is often referred as the optimum blowing ratio. The optimum-blowing ratio for a row of 30° jets is around 0.5, and relatively less for a row of 60° jets. The other findings were that the effectiveness varied in the lateral direction up to x/D of 10 and that the effects were more pronounced for high blowing rates and large pitch-to-diameter ratios. The centreline effectiveness was always higher than that at the lateral distances from the centre of the hole. Comparisons between current results and those of other researchers are discussed in Section 4.

Pietzyk et al. [15] studied a row of 35° jets with a length-to-diameter ratio of 3.5 and a pitch-to-diameter ratio of 3, and found that the disturbance added by the multiple jets increased the turbulence intensity, the turbulence length scale for the row of jets was smaller than that of a single jet, and the vortex systems responsible for mixing were able to re-entrain the warmer fluid from the neighbouring jets.

Sinha et al. [16] studied two rows of 35° holes with a pitch-to-diameter ratio of 3 and a row spacing-to-diameter ratio of 40, and showed that the upstream row thickened the boundary layer between the two rows, reduced the momentum of the crossflow and the velocity in the shear layers, and lowered the turbulence level for the second row. They also found that the jets from the downstream row extended further from the wall and penetrated deeper into the mainstream than their first row because the jets from the second row were diverted less by the approaching flow due to the greater momentum deficit of the approaching flow at the second row. Jubran and Brown [17] suggested that effectiveness downstream of a second row of jets was dependent on the state of the development of the film from the first row, and its development length increased with increasing row spacing, which subsequently resulted in a near two-dimensionality when the downstream row was encountered.

The current study extends the scope of the previous investigation of Yuen and Martinez-Botas [1,2] using the same wide band liquid crystal thermography and the steady state heat transfer method to provide two-dimen-

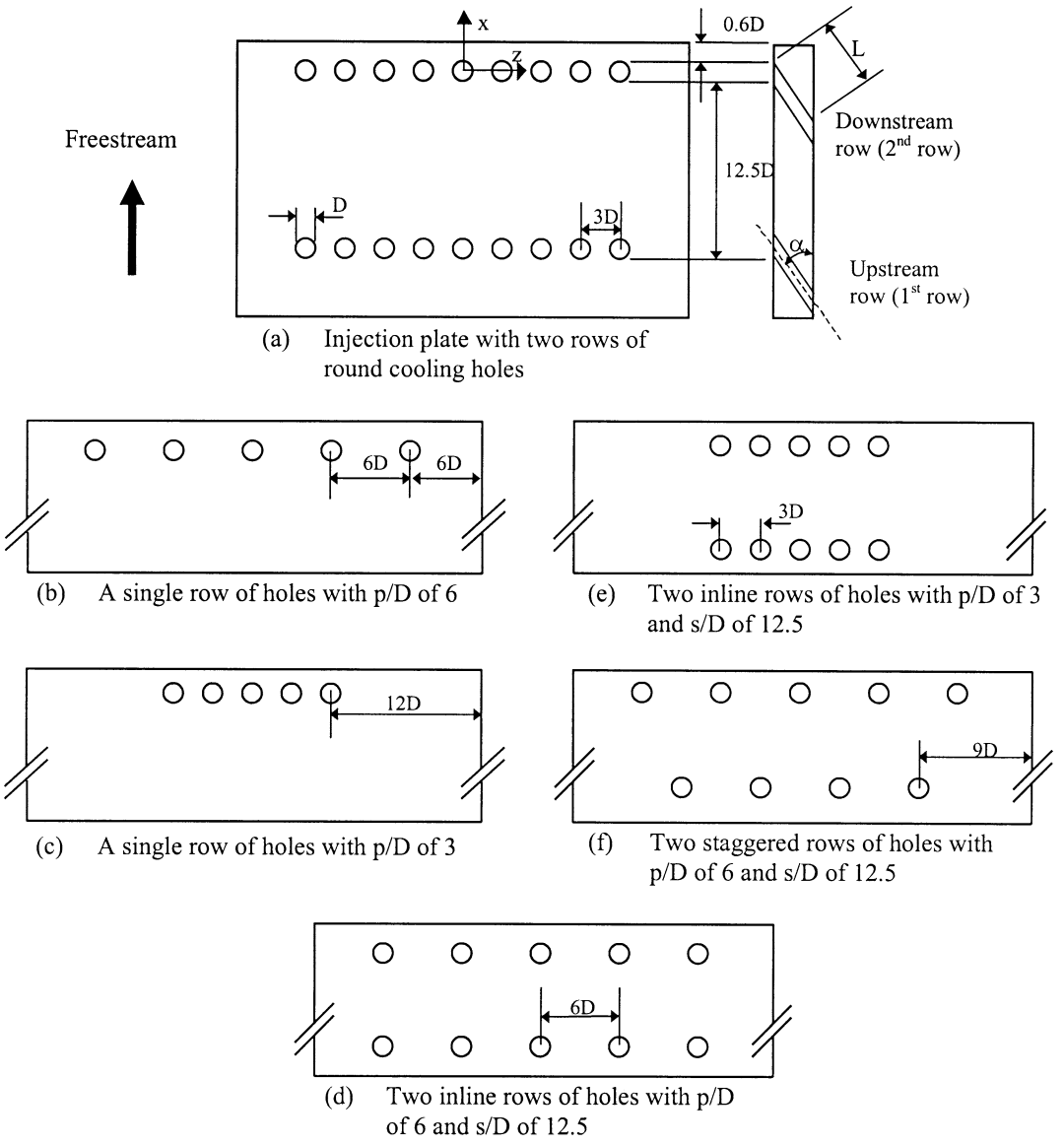

Fig. 1. Geometries and arrangements of cooling holes at steamwise angle, α.

sional surface plots of effectiveness for single, inline and staggered rows of round holes at three streamwise angles shown in Fig. 1, with good spatial resolution. The studies of Yuen and Martinez-Botas [1,2] provided some insight to the film cooling performance of a single cooling hole, and serve as a benchmark to which the more complex geometries with jet-to-jet interactions are added.

2. Characteristics of jets in a crossflow

Margason [18] reviewed extensively the study of film cooling. Yuen and Martinez-Botas [1] and Yuen [19] reported some of the findings, only a small proportion of which is described here. Bergeles et al. [20] and Crabb et al. [21] found that the velocity profile across the exit plane of a single vertical jet can be non-uniform and more so with low blowing ratios. Andreopoulos and Rodi [22] found that the crossflow acted like a partial cover over the exit with a blowing ratio of 0.5, and caused the flow inside the hole to exit near the downstream side with greater velocity than the freestream.

Walters and Leylek [23] verified that the non-uniform distribution of jet profile with the single vertical jet obtained by researchers [9,21,22,24], was present with the 35° jet, and suggested that its extent depended on the length-to-diameter ratio of the pipe which transported

the jet fluid, blowing ratio and geometry. The length-to-diameter ratio of the pipe used by Bergeles [9], Andreopoulos and Rodi [22] and Pietrzyk et al. [24] was 50, 12 and 3.5, respectively. The fluid in the film hole shifted towards the trailing edge at low blowing ratios, and was pushed towards the leading edge at large blowing ratios.

The effects of the separated flow inside the cooling hole had less time to attenuate as the length-to-diameter ratio decreased, and exerted more influence on the jet exit conditions.

3. Experimental apparatus and procedure

The present investigation is a continuation of the study on the single round hole of Yuen and Martinez-Botas [1,2], and therefore is carried out using the same wind tunnel, test facility, measurement technique which is the wide band crystals and the steady state heat transfer method, imaging and processing procedures. The details are given in Yuen and Martinez-Botas [1] and Yuen [19], and will only be briefly described here for the sake of completeness.

The encapsulated liquid crystal used in current study offers a bandwidth of 10 °C. The test rig has a modular design, and is presented in Fig. 2. Three injection plates were made of Perspex, and each plate contained two rows of nine cylindrical holes with streamwise inclinations of 30°, 60° and 90° and a row spacing of 12.5 diameters, Fig. 1. For the cases with one row, the upstream row was covered with thin tape, and the appropriate holes in the downstream row were also covered to deliver the required pitch-to-diameter ratio. For all test cases, each row of jets stemmed from five cooling holes, except for the upstream row of the two staggered rows, which had four, Fig. 1. Thus, the hole furthest from the centreline of the working section was located at twelve diameters with a pitch-to-diameter ratio of 3, six diameters with a pitch-to-diameter ratio of 6, and nine diameters for the upstream staggered row, with a pitch-to-diameter ratio of 6 from the side-walls of the tunnel for the three cases and it was unlikely that the wall interfered with the spreading of the jets. The laterally averaged values of effectiveness were taken across one pitch across the central hole. The downstream row of holes were positioned as close as possible to the downstream edge of the injection plate, such that the trailing

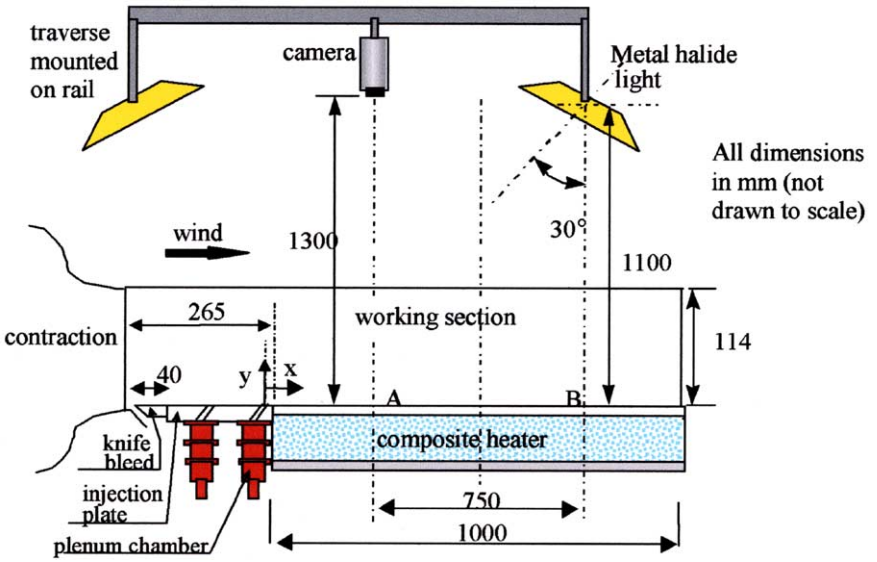

Fig. 2. Experimental set-up.

Table 1
Test cases (105 in total)

Streamwise angles (°)	Configurations	No. of blowing holes in each row	p/D	s/D	Blowing ratio (M)
30, 60 and 90	One row	5	3 and 6		0.33, 0.5, 0.67, 1.0, 1.33,
	Two-inline rows			12.5	1.67 and 2.0
	Two-staggered row	Four in the upstream row	6		
		Five in the downstream row			

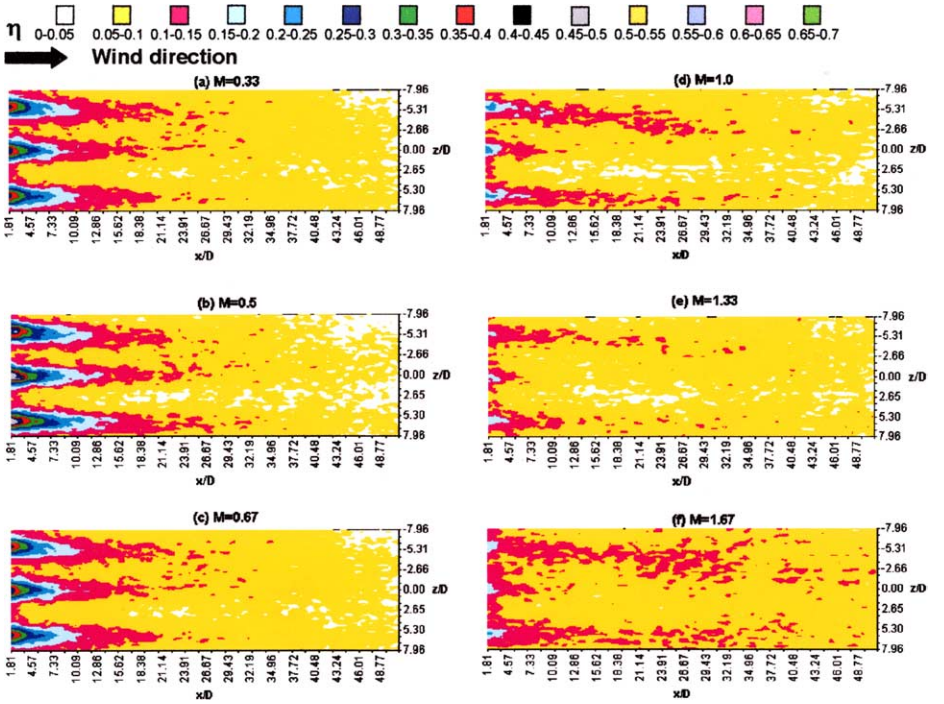

Fig. 3. Film cooling effectiveness for a row of 30° holes with p/D of 6 (only the centre 3 are shown).

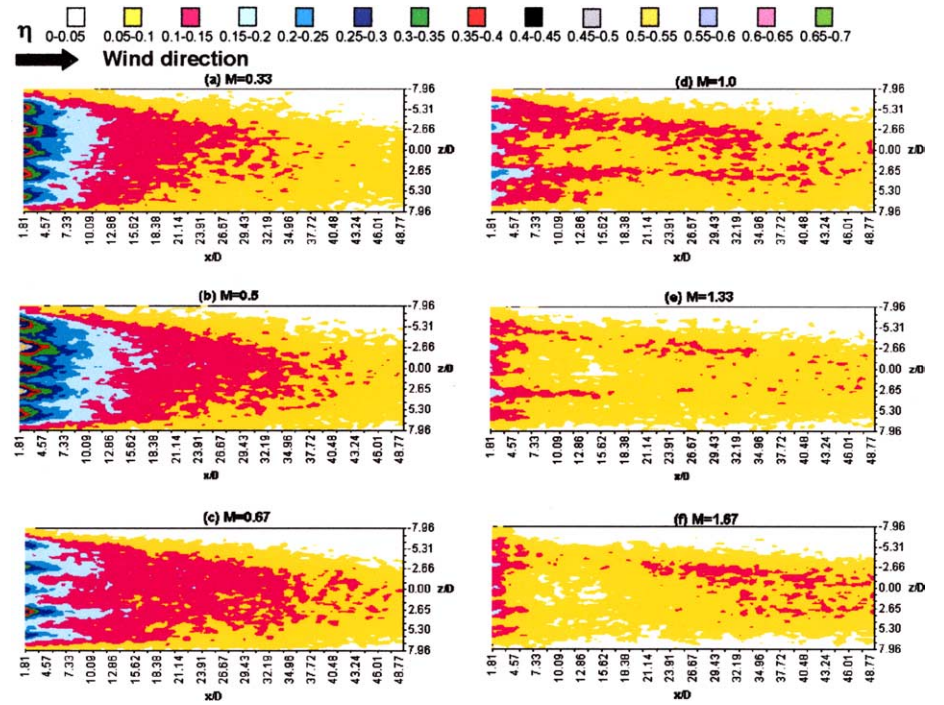

Fig. 4. Film cooling effectiveness for a row of 30° holes with p/D of 3.

edge of the holes was 6 mm from the downstream edge of test plate, which was desirable from the view point of measurements.

The composite test plate is 360 mm wide × 1000 mm long × 163 mm thick, and is well insulated by a 10 mm thick Tufnol sheet, which has good thermal resistance and mechanical strength and a 150 mm thick Styrofoam block, to approximate a near-adiabatic wall. Details of the test plate are given in Yuen and Martinez-Botas [2,3] and Yuen [19]. Ten T-Type (copper–constantan, standard gage 39–40) thermocouples were installed under the uppermost layer (stainless steel sheet).

The imaging system comprised of a colour JVC CCD camera, two light sources, and a 24-bit frame grabber installed in a computer. The temperature and hue calibration for the liquid crystals was performed on the actual test surface, without the crossflow or injectant. Once surface temperature and colour had stabilised, the images for the calibration and the actual tests were at 25 frames/s captured by the CCD camera, the corresponding temperatures from the thermocouples were recorded by two analogue to digital modules which were calibrated with a precise voltage source and utility software with cold junction compensation incorporated. The accuracy of the calibrated thermocouples is ±0.5 °C. The images captured were then converted from the RGB to HSI format. In the current investigation, 1968 frames were used in each calibration. The camera settings, light source, distance, and angle were kept the same for both the calibration and actual experiments. The calibration procedure was repeated three times during the whole series of test cases, the results showed no calibration drift.

3.1. Experimental uncertainty

The conduction errors were analysed for one row of holes with a streamwise inclination of 30° and a pitch-to-diameter ratio of 3 at a blowing ratio of 0.5, and were calculated to be less than 10%. Uncertainties are evaluated by the method of Kline and McClintock [25]. Corrections are applied to consider heat loss through thermocouple leads using the method proposed by Schneider [26]. The uncertainty in η is approximately ±9%.

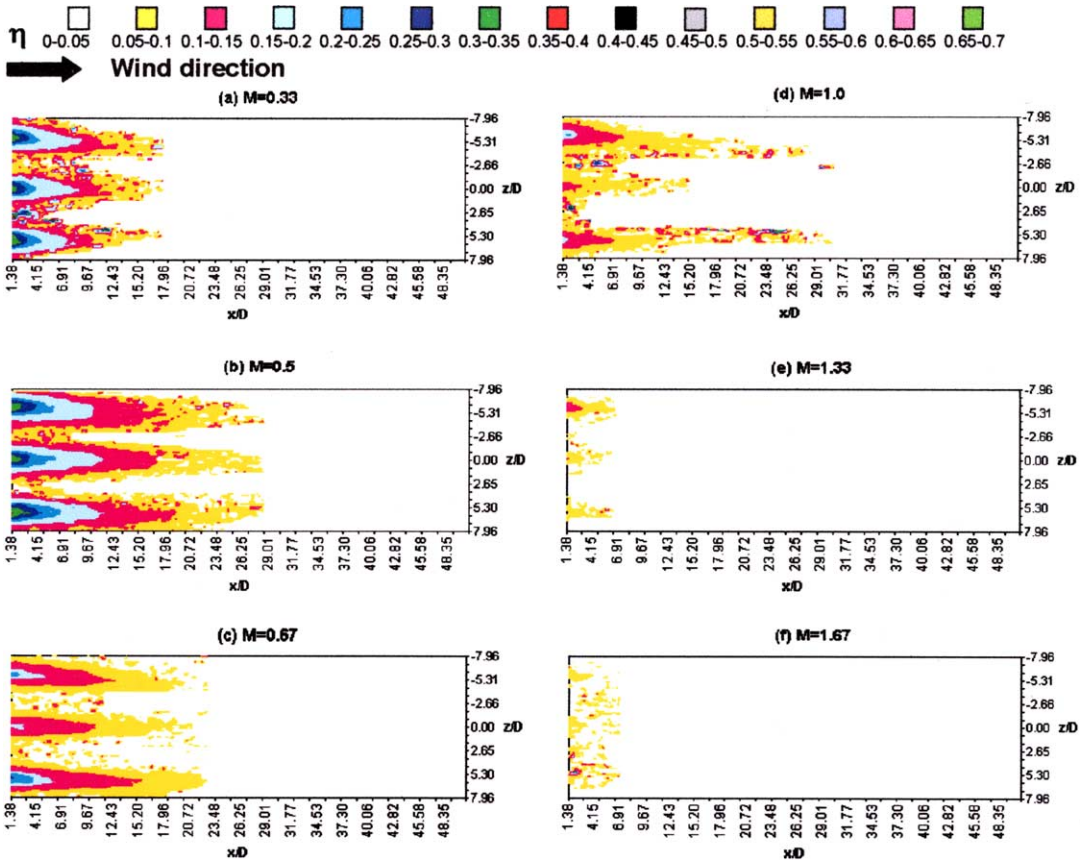

Fig. 5. Film cooling effectiveness for a row of 60° holes with p/D of 6 (only the centre 3 are shown).

3.2. Operating conditions

The freestream velocity was maintained at 13 m/s, the corresponding Reynolds number based on the hole diameter and freestream velocity, Re_D, was 8563. The freestream temperature and the turbulence intensity were 20 °C and 2.7%, respectively, and the injectant-to-freestream blowing ratio varied from 0.33 to 2. The turbulence measurements of free stream conditions indicated that the integral length scale was 28.6 mm. The conditions at the hole exit were measured with a small pitot probe to see the distribution of the exit profile, it was found that the profile was near a top-hat variation for the high blowing ratios, there was not enough spatial resolution to provide sufficient quantitative results; note the short to length-to-diameter ratio use in the current experiment. The effectiveness tests were conducted with the test plate unheated to approximate an adiabatic surface; the injectant was heated by an in-line heater to 40 °C ($\rho_2/\rho_\infty = 0.92$). The jet temperature was measured by a T-type thermocouple at the hole exit and in the plenum chamber. The difference between these temperatures was approximately 0.1 °C. The injectant temperature refers to that at the hole exit. The test cases investigated in the current study are listed in Table 1.

In the absence of jets, the freestream boundary layer thickness grows from approximately $\delta/D = 0.1$ at $x/D = -24.8$ (see Figs. 1 and 2 for the location of the measuring axis) to approximately $\delta/D = 1.0$ at the downstream row of holes ($x/D = 0$). The displacement thickness (δ^*/D) and momentum thickness (δ_i/D) are 0.15 and 0.11, respectively at the plane of injection from the downstream row.

4. Results

In the results presented here, the axial range is classified into four regimes for clarity: the immediate region for $x/D \leqslant 3$, the near field for $3 \leqslant x/D \leqslant 7$, the intermediate region for $7 \leqslant x/D \leqslant 26$, and the far downstream region for $x/D \geqslant 26$.

4.1. One row of 30° holes

Fig. 3 illustrates the film cooling effectiveness from the three central jets with a pitch-to-diameter ratio of

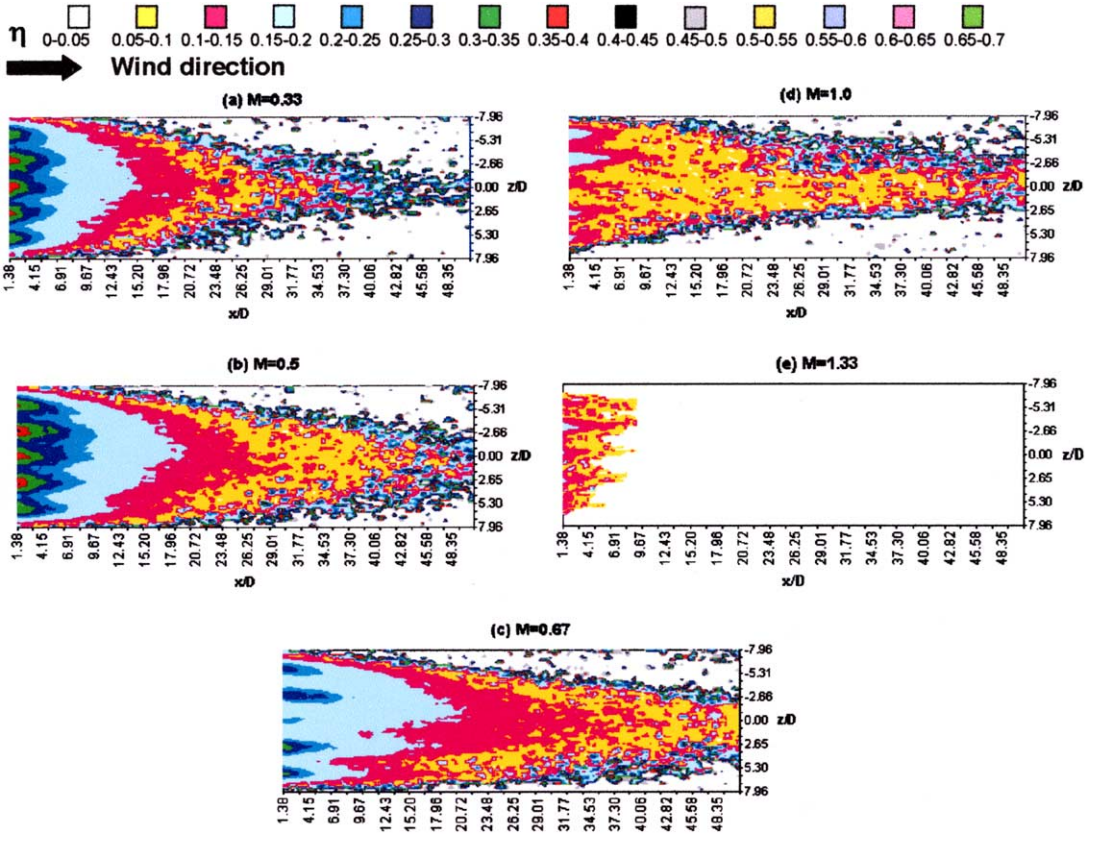

Fig. 6. Film cooling effectiveness for a row of 60° holes with p/D of 3.

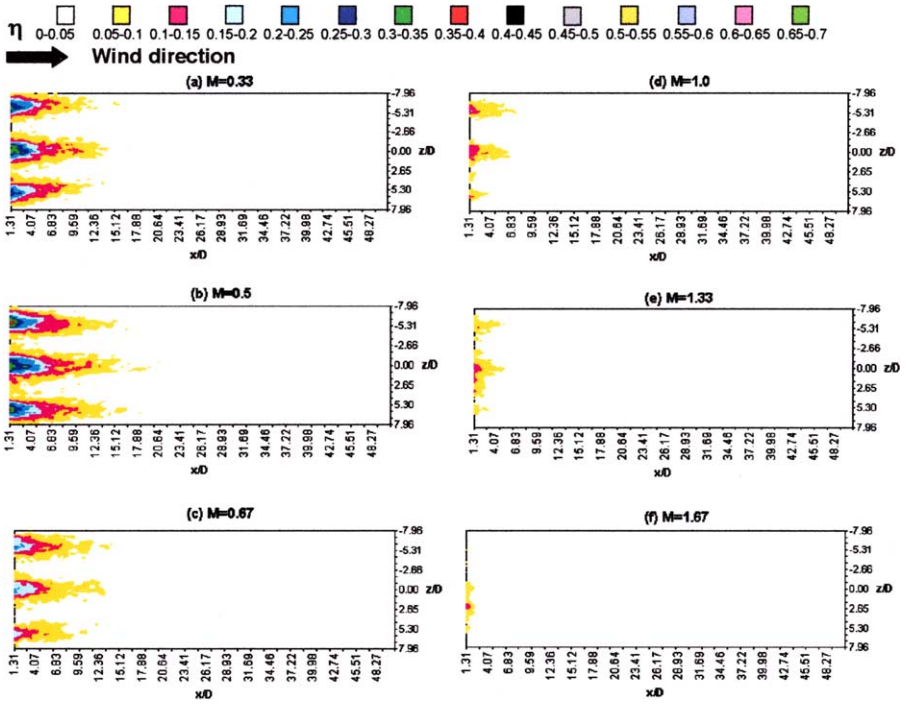

Fig. 7. Film cooling effectiveness for a row of 90° holes with p/D of 6 (only the centre 3 are shown).

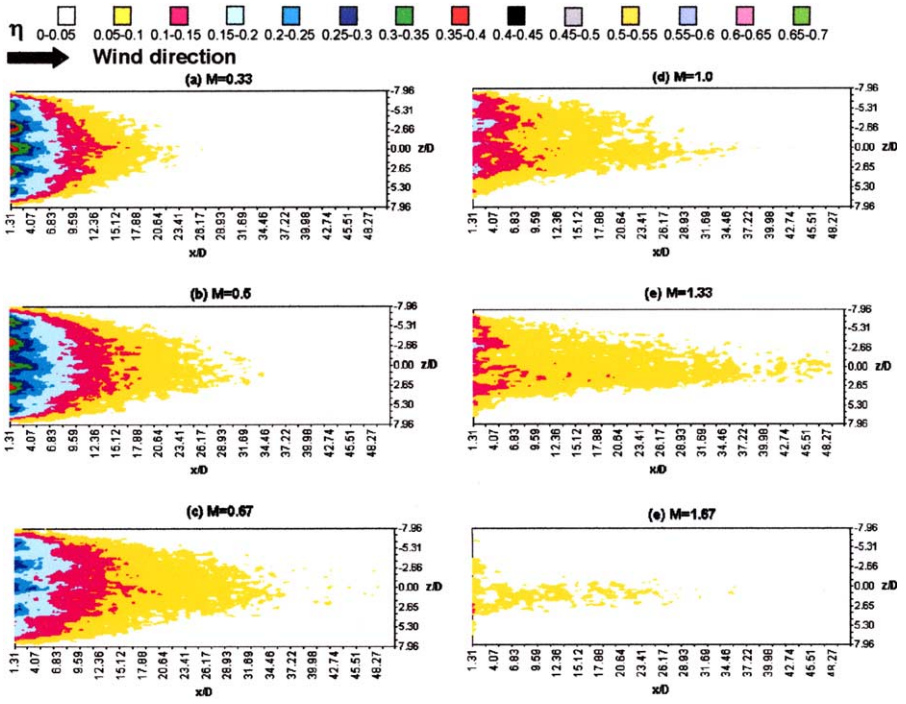

Fig. 8. Film cooling effectiveness for a row of 90° holes with p/D of 3.

6 with blowing ratios in the range from 0.33 to 1.67. The direction of crossflow is from left to right, the axial position for the row of holes was the same as that for a single hole in Yuen and Martinez-Botas [1], with x/D originating from the centre of the hole, and z/D from the centreline of the centre hole, Fig. 1, and the chosen interval of η is 0.05. The asymmetric scatter far downstream, where $0 \leqslant \eta \leqslant 0.1$, fell within the uncertainty band discussed. The spreading of the individual jets was similar to that of a single jet in Yuen and Martinez-Botas [1] for x/D less than 7 and blowing ratios less than unity, and the centreline distributions of effectiveness were marginally larger than those with a single hole for all axial locations and blowing ratios. The effectiveness between the jets suggests some interaction for x/D greater than 7, which is surprising even though the effective diameter was larger than the hole diameter due to the vortical flow around the jet, with decrease in effective pitch-to-diameter ratio. On the other hand, the velocity between the jets was probably higher than that with the single jet of Yuen and Martinez-Botas [1], and this may have been responsible for the larger effectiveness. Resolution of the related uncertainty requires extensive consideration of the three-dimensional flow between the jets and this was beyond the scope of this investigation. The row of holes with a pitch-to-diameter ratio of 6 provided an uniform effectiveness coverage in the far downstream region, and the difference between the single 30° hole and the row of 30° holes with a pitch-to-diameter ratio of 6 increased at high blowing ratios, $M \geqslant 1$, which was due to growing jet interaction with downstream distance.

Fig. 4 shows the distribution of effectiveness with one row of 30° holes and a pitch-to-diameter ratio of 3. The centreline effectiveness distributions are similar to those with a row of jets with a pitch-to-diameter ratio of 6 for x/D less than 10, and thereafter the coverage and values increased with the smaller pitch-to-diameter ratio due to the increased jet interaction. The effectiveness along the axis of the outer jets tended to be lower although the distance from the axis of the jet to the edge of the displacement thickness of the side-wall boundary layer was approximately 11.8

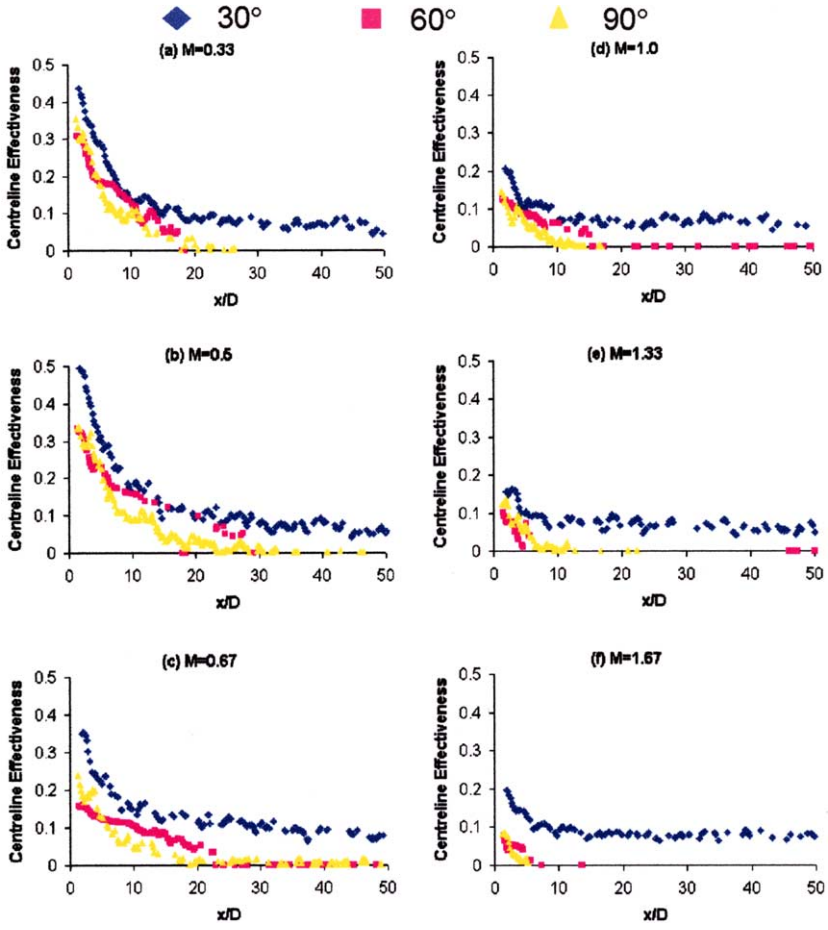

Fig. 9. Effects of streamwise angle on centreline effectiveness for a row of holes with p/D of 6.

diameters at x/D of 7. This effect was not observed with the higher pitch-to-diameter ratio with which the corresponding distance was 5.8 diameter, which may be due to the fact that a larger proportion of the freestream may have accelerated between the adjacent jets. The study of the furthest holes is of interest to assess the final cooling hole of a row, since there is a significant deterioration in performance.

Fig. 4 shows an effectiveness of around 0.2 at mid-span with a blowing ratio of 0.5 in the immediate and near field regions. This is larger than that of Goldstein et al. [6], Jabbari and Goldstein [7], Cho et al. [27] and Yu et al. [28], who reported a value of 0.1 for similar conditions. On the other hand, Han and Mehendale [12], Vedula and Metzger [13], and Ekkad and Han [14] reported an effectiveness of 0.2 close to mid-span for a row of 30° holes with a blowing ratio of 0.5 and with similar experimental methods. The mid-span effectiveness was probably affected by the jet and freestream flow characteristics, and in common with the arguments made in relation to the higher pitch-to-diameter ratio. Baldauf et al. [29] found the not-surprising result that increased turbulence enhanced jet and mainstream interaction and resulted in a more rapid tendency for equalisation of lateral temperatures. This mid-span effectiveness value raises the question of conduction effects, and the lateral temperature gradient was calculated to be much less than that in the y-direction (less than 10% for the worst case). The results of Pedersen et al. [8] are similar to those reported here and were obtained with a mass transfer method that was not subject to heat transfer uncertainties. This provides support for rapid mixing of jet fluid with the flow between the jets, perhaps due to the vortical structures and the small effective pitch-to-diameter ratios.

4.1.1. At 60° and 90°

Fig. 5 shows the distribution of effectiveness with a single row of 60° holes and a pitch-to-diameter ratio of 6, which produced similar centreline effectiveness val-

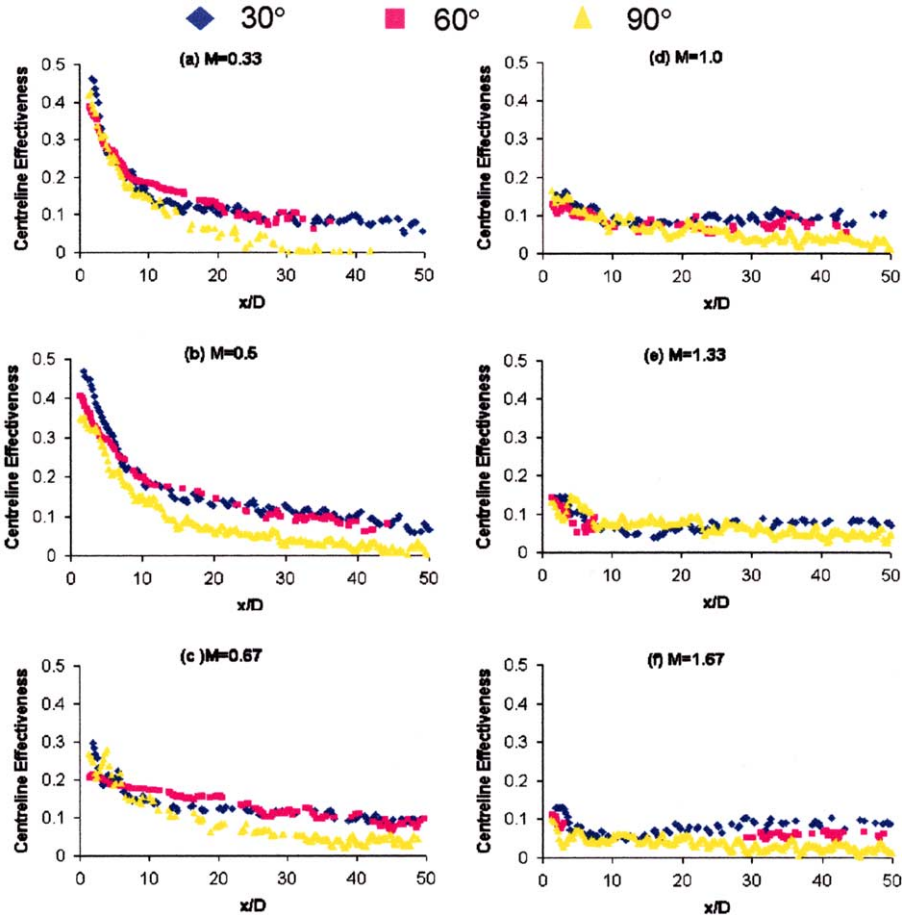

Fig. 10. Effects of streamwise angle on centreline effectiveness for a row of holes with p/D of 3.

ues to those with a single 60° hole in the previous study by Yuen and Martinez-Botas [1]. Fig. 6 presents the distribution of effectiveness with a single row of 60° holes and a pitch-to-diameter ratio of 3, which shows that the smaller pitch has increased the values on the centreline and at finite radii. Figs. 7 and 8 show the distributions of effectiveness for a single row of 90° holes with two pitch-to-diameter ratios. The row with a pitch-to-diameter ratio of 6 produced an almost identical effectiveness distribution to that with the single 90° hole of Yuen and Martinez-Botas [1], and the smaller pitch increased the coverage and values. The effects of injection angle and pitch-to-diameter ratios are discussed in the following sections.

4.1.2. Effects of hole angle

Fig. 9 assembles the variations of centreline effectiveness with axial distance for a pitch-to-diameter ratio of 6 and the three injection angles tested. The single row of 30° holes gave rise to larger values than the steeper holes at a given axial position, pitch-to-diameter ratio and blowing ratio.

The trend of $\eta_{30°} > \eta_{90°} > \eta_{60°}$ in the near field region with the single hole observed in Yuen and Martinez-Botas [1] was observed here with a row of holes, a pitch-to-diameter ratio of 6 and a blowing ratio of 0.33, Fig. 9a. It is worth noting that in the current set of experiments this trend was retained even very close to the hole (immediate region of $x/D < 3$) which was

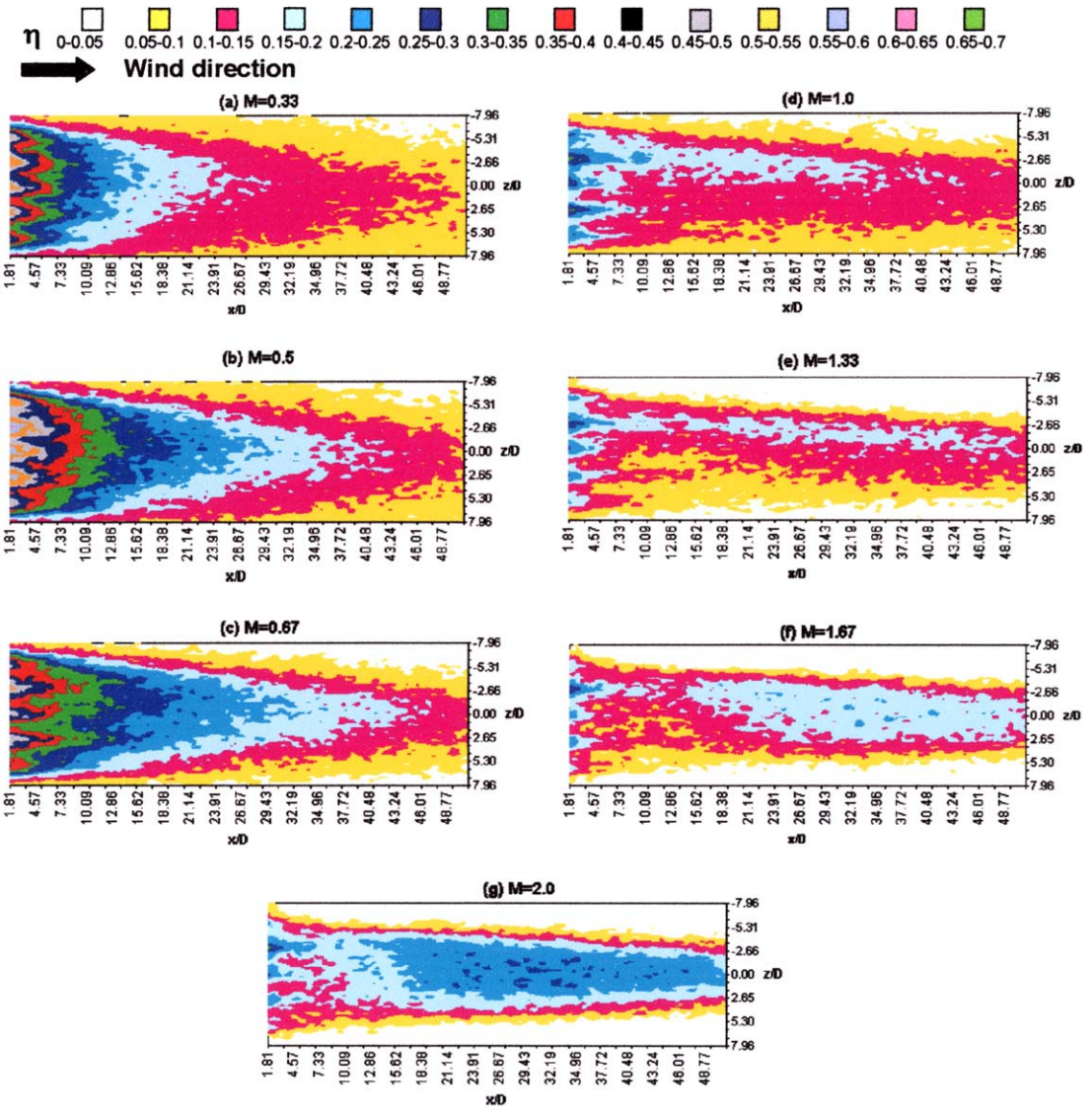

Fig. 11. Film cooling effectiveness for two inline rows of 30° holes with p/D of 3 and s/D of 12.5.

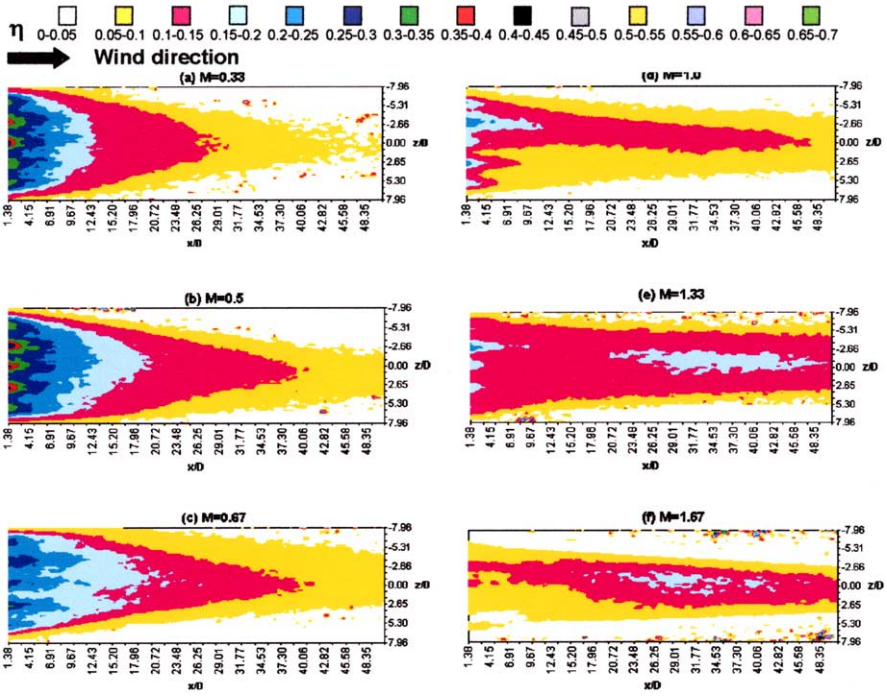

Fig. 12. Film cooling effectiveness for two inline rows of 60° holes with p/D of 3 and s/D of 12.5.

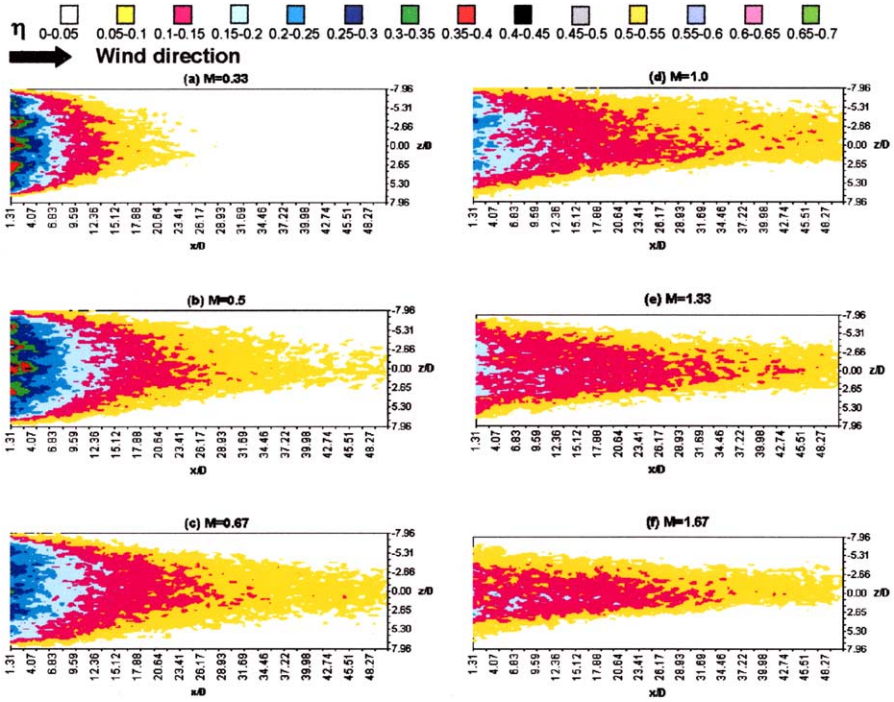

Fig. 13. Film cooling effectiveness for two inline rows of 90° jets with p/D of 3 and s/D of 12.5.

not the case in a single hole [1] where the more traditional trend of $\eta_{30°} > \eta_{60°} > \eta_{90°}$ was measured; clearly the jet-to-jet interaction is responsible of this trend reversal. Baldalf et al. [29] found a similar trend, and attributed this to the early injectant interaction initiated by immediate spreading and subsequent merging of the adjacent warm 90°.

Fig. 9b illustrates the distribution of centreline effectiveness with a single row of holes and a pitch-to-diameter ratio of 6 at a blowing ratio of 0.5 for the three angles. The row of 30° holes provided larger effectiveness than the row of 60° or 90° holes, especially for the immediate and near field regions. The trends found with blowing ratios equal to, or greater than, unity in Fig. 9d–f are similar to those with the corresponding single jet comparison of the previous work of Yuen and Martinez-Botas [1].

4.1.3. Effects of hole spacing

Comparison between Figs. 3 and 4 for the row of 30° holes with pitch-to-diameter ratios of 6 and 3, respectively, shows that the smaller pitch gave similar centreline effectiveness to the larger pitch with a row of 30° holes, but increased the coverage with effectiveness greater than 0.15 by 75% for blowing ratios below unity. Furthermore, the spanwise variation in effectiveness diminished with the smaller pitch as the jets provided more complete coverage, particularly for the immediate and near field regions. This observation was also found in the comparison between Figs. 5 and 6 for rows of 60° holes and between Figs. 7 and 8 for rows of 90° holes with pitch-to-diameter ratios of 6 and 3, respectively. Khan and Whitelaw [30] reported that multiple jets acted as a single jet with a common recirculation zone when the pitch-to-diameter ratio was small.

Fig. 10 presents the distributions of centreline effectiveness with one row of holes and a pitch-to-diameter ratio of 3 at the three angles. The closer hole-spacing increased the effectiveness by an average of 20% with the row of 60° holes in the immediate region for blowing ratios below unity, and by 100% away from the holes ($x/D \geqslant 16$) for all blowing ratios. For the row of 90°

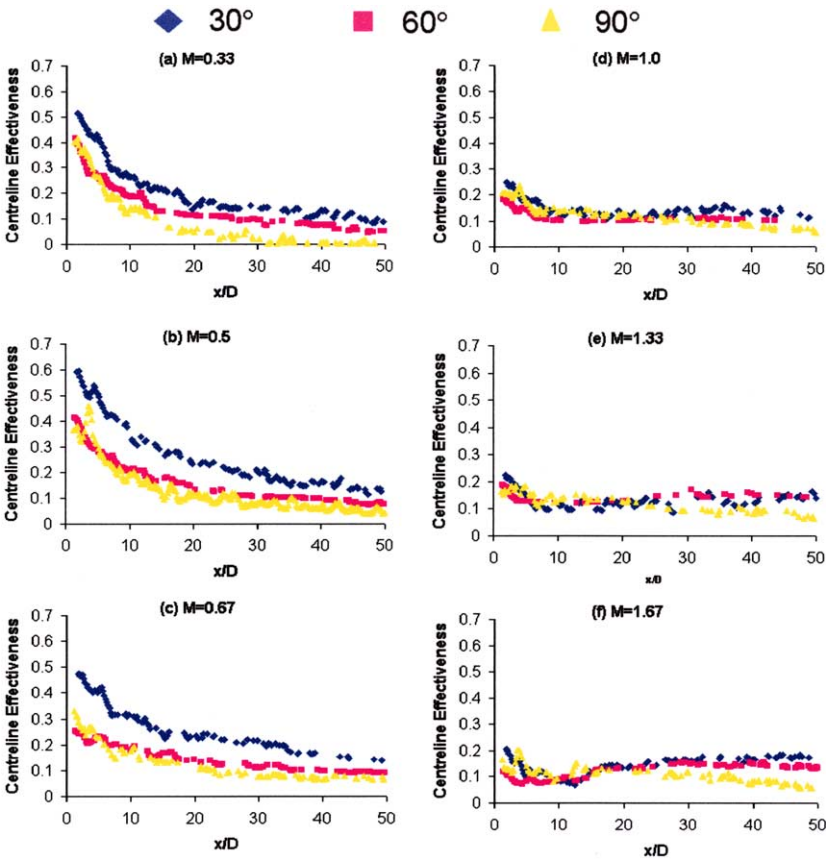

Fig. 14. Effects of streamwise angle on centreline effectiveness for two inline rows of holes with p/D of 3 and s/D of 12.5.

holes, the smaller pitch gave similar centreline values to the larger pitch in the vicinity of the holes, but increased the centreline values by 100% away from the holes.

The 60° holes gave larger effectiveness values than the 30° and 90° holes at a blowing ratio of 0.67 in the near field and intermediate regions. This unexpected result has also been reported by Foster and Lampard [31], who compared 35° and 60° holes. The review of the influence of the length-to-diameter ratio of the duct leading to the jet exit described earlier and in Yuen and Martinez-Botas [1] and Yuen [19], discussed variations of the static pressure gradient across the hole exit. The resulting jet velocity profile and variation in shear around the periphery of the 30°, 60° and 90° holes could be the cause of this trend.

4.2. Two rows of holes

4.2.1. At 30°

Fig. 11 provides contour plots of effectiveness with two-inline rows of 30° holes with a pitch-to-diameter ratio of 3. The origin of x/D remained at the centre of

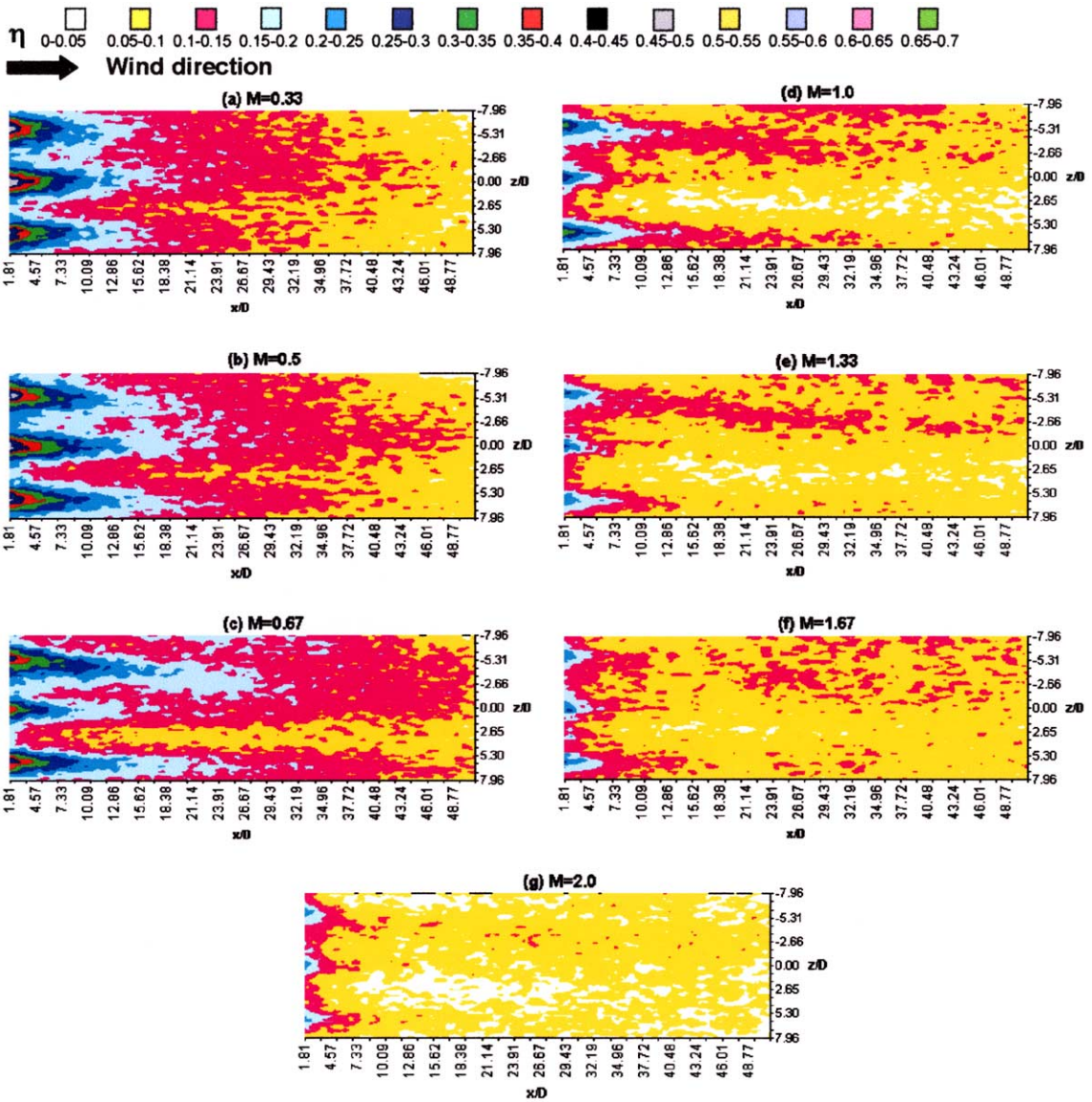

Fig. 15. Film cooling effectiveness for two inline rows of 30° holes with p/D of 6 and s/D of 12.5 (only the centre 3 are shown).

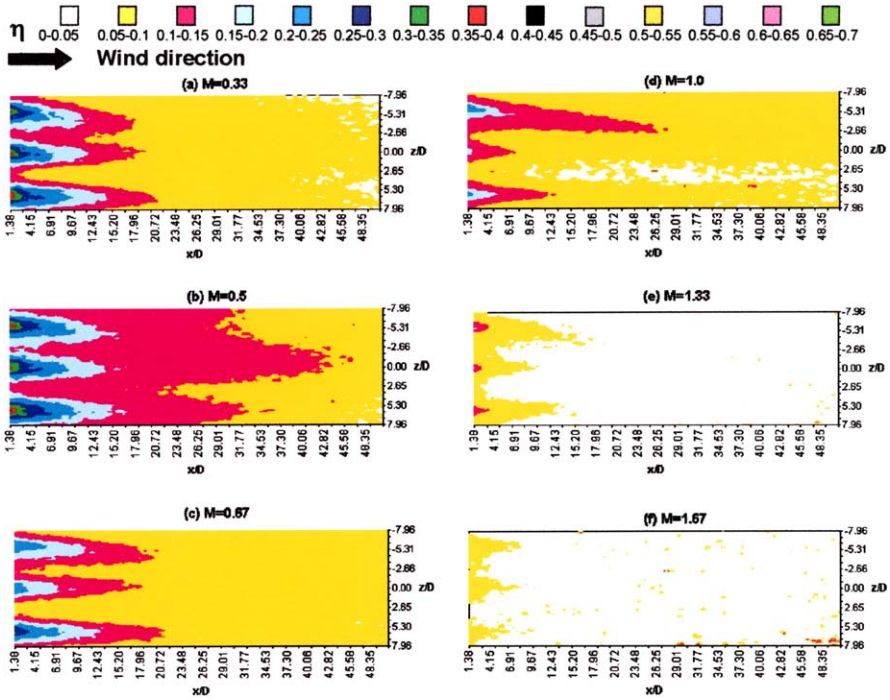

Fig. 16. Film cooling effectiveness for two inline rows of 60° holes with p/D of 6 and s/D of 12.5 (only the centre 3 are shown).

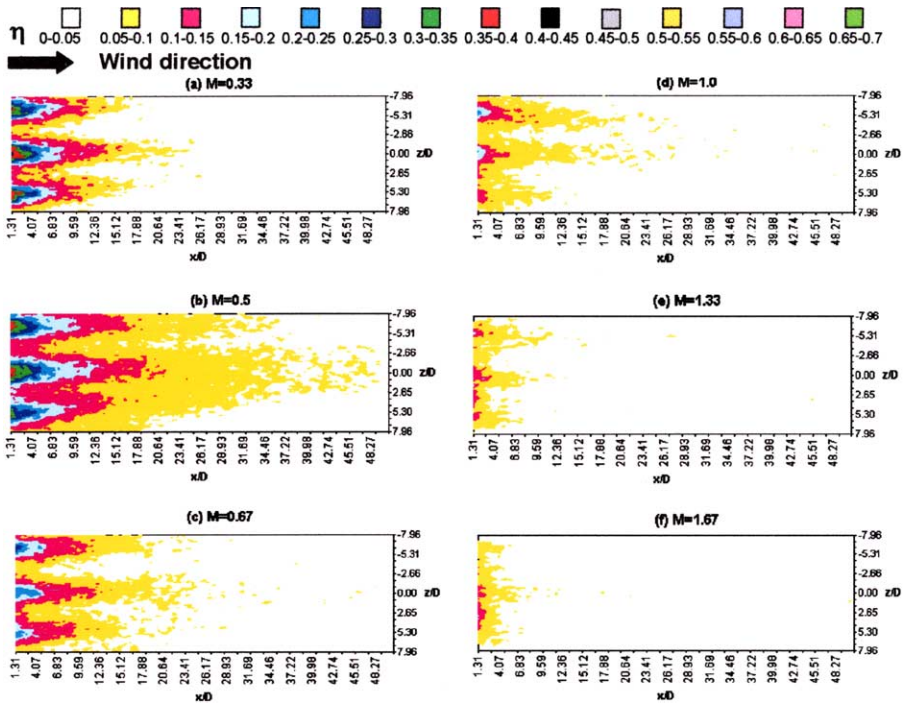

Fig. 17. Film cooling effectiveness for two inline rows of 90° holes with p/D of 6 and s/D of 12.5 (only the centre 3 are shown).

the hole in the downstream row with z/D from the centreline of centre hole in the downstream row. The upstream inline row increased the effectiveness values and coverage by up to 100% in the immediate and near field regions, which was expected since the two rows provided twice as much injected mass flow as the single row at a given blowing ratio.

The results of Fig. 11a for two-inline rows of 30° holes at a blowing ratio of 0.33 may be compared to those of Fig. 4c, which were obtained with one row of 30° holes of the same pitch at a blowing ratio of 0.67 for the equivalent injected mass flow. Comparison between Figs. 4 and 11 show that the two rows were advantageous for all blowing ratios since the upstream row may redirect the downstream jets and increase the temperature gradient in the vertical direction at a given streamwise location, with the added advantage of cooling the surface between the two rows.

4.2.2. Effects of hole angle

Figs. 12 and 13 provide contour plots of effectiveness with two-inline rows and a pitch-to-diameter ratio of 3 for the 60° and 90° holes, respectively. The single and two-inline rows of 60° holes, Figs. 6 and 12, and of 90° holes, Figs. 8 and 13, show that the upstream row helped the second row of jets to remain closer to the wall for blowing ratios greater than 0.33 and this occurred with the same blowing ratio and with the same injected mass. The axial shrinkage and lateral stretching of the effectiveness coverage with increasing angle were also present with the two-inline rows, which is consistent with the findings of Eriksen and Goldstein [4].

Fig. 14 shows the distribution of the centreline effectiveness with two-inline rows of holes and a pitch-to-diameter ratio of 3 at the three angles. The 30° holes gave the largest values for blowing ratios equal to, or less than 0.67, again because they turned more easily towards the wall than those with larger angles. Further increases to blowing ratios of 1 and 1.33 brought the effectiveness values closer together for all three angles, and the two-inline rows of 30° jets no longer provided the largest effectiveness. This suggests that the upstream row could do little to redirect the downstream row at large blowing ratios.

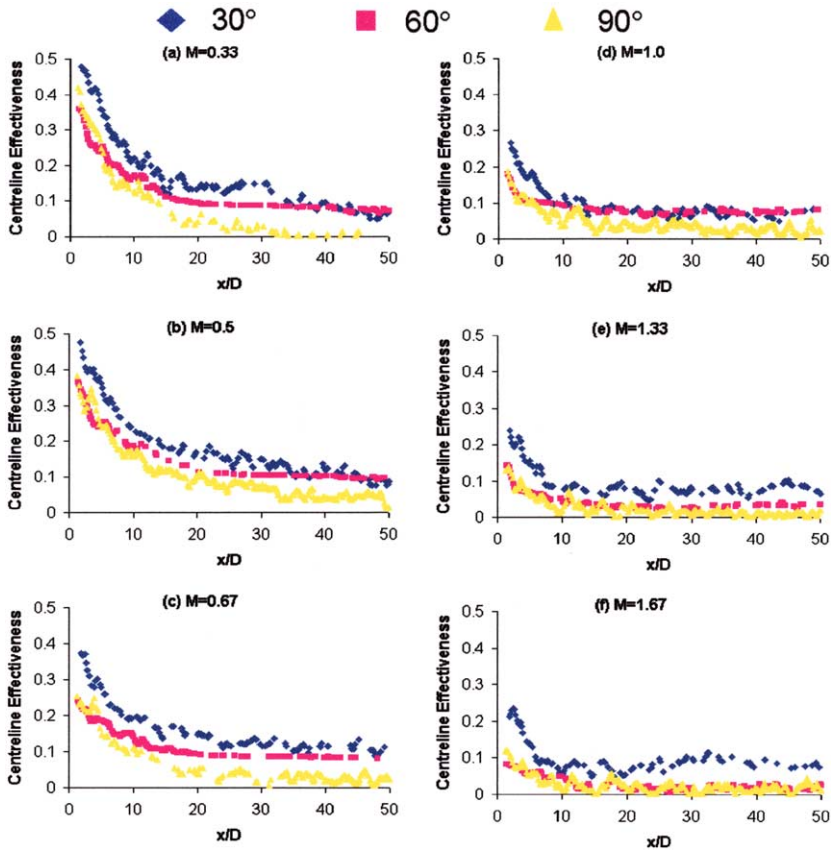

Fig. 18. Effects of streamwise angle on centreline effectiveness for two inline rows of holes with p/D of 6 and s/D of 12.5.

4.2.3. Effects of hole spacing

Fig. 15a–g presents the distribution of effectiveness with two-inline rows of 30° holes and a pitch-to-diameter of 6. The film coverage was less than that with two-inline rows of 30° holes and a pitch-to-diameter ratio of 3, for which Fig. 11 shows that the acceleration around the row of holes was significant, and the spanwise variation in effectiveness was smaller. Comparison with the corresponding single row of 30° holes and a pitch-to-diameter ratio of 6 in Fig. 3 revealed that the upstream inline row increased effectiveness coverage for constant injected mass flow and for the same blowing ratio. The maximum effectiveness near the holes occurred at a blowing ratio (M of 0.67) greater than that with a single row (M of 0.5), which may suggest that the upstream row helped the downstream row to remain close to the wall until a larger blowing ratio was introduced.

Figs. 16 and 17 show the distributions of effectiveness for two-inline rows with a pitch-to-diameter ratio of 6 for the 60° and 90° holes, respectively. Results with

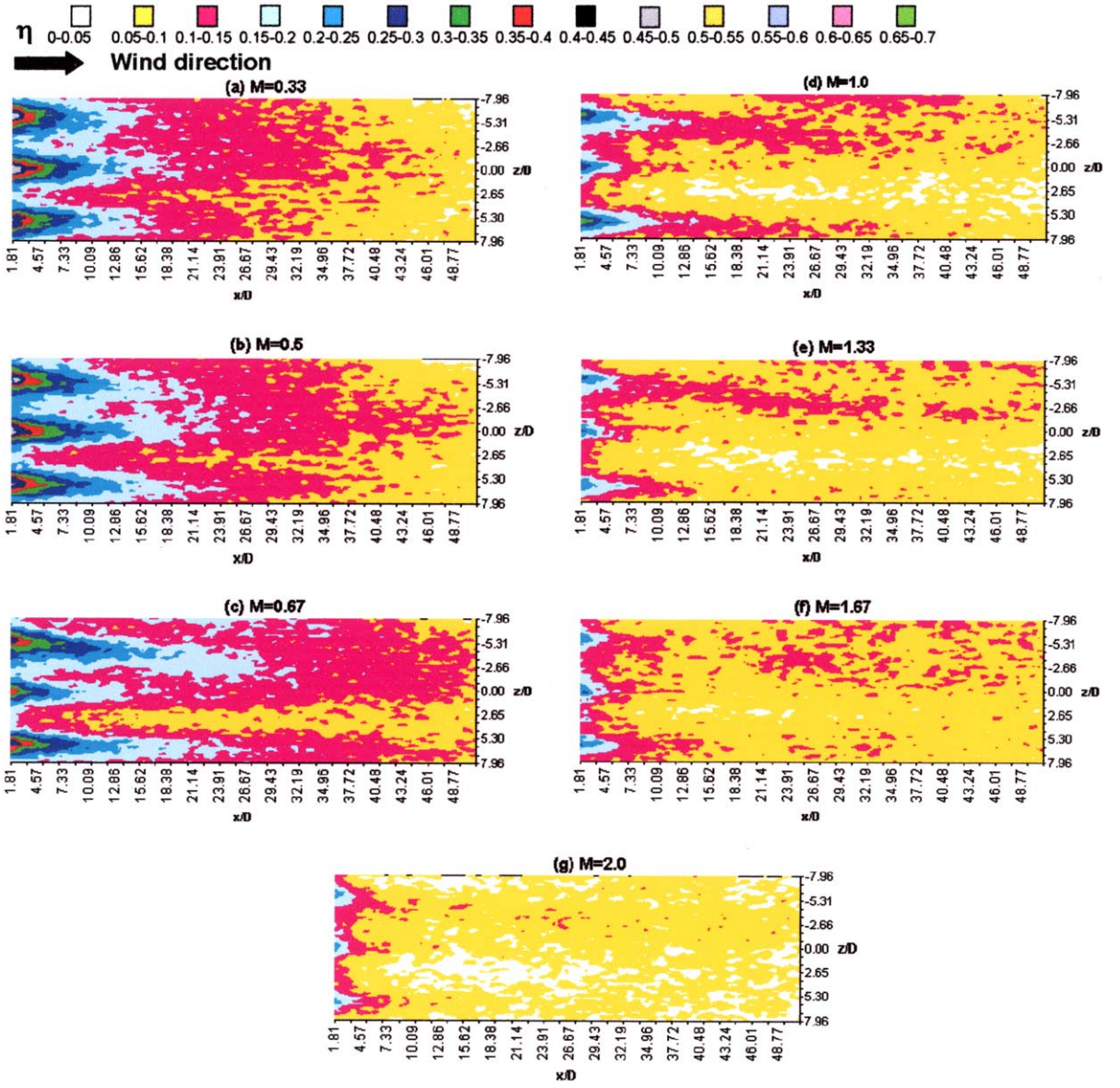

Fig. 19. Film cooling effectiveness for two staggered rows of 30° holes with p/D of 6 and s/D of 12.5 (only the centre 3 are shown).

the single row of the same pitch are shown in Figs. 5 and 7 for the 60° and 90° holes, respectively. The two rows of 60° and 90° holes gave larger effectiveness and coverage for the same blowing ratio and injected mass flow, as with the 30° holes.

Fig. 18a–f shows the distributions of centreline effectiveness with two-inline rows and a pitch-to-diameter ratio of 6 for the three angles. The shallowest holes consistently gave larger values for a wide range of axial locations and blowing ratios, similar to the findings with the inline rows with a pitch-to-diameter ratio of 3, in Fig. 14. Comparison between Figs. 9 and 18 shows that the effect of the upstream row was insignificant with a pitch-to-diameter ratio of 6 for blowing ratios equal to, or less than 0.67, and only became apparent with blowing ratios greater than 0.67 for all three angles. The two-inline rows with a pitch-to-diameter ratio of 6 at the three angles, Fig. 18b, gave smaller centreline values than the inline rows with a pitch-to-diameter ratio of 3 and a blowing ratio of 0.5, Fig. 14b.

Figs. 19–21 show contours of effectiveness with the two staggered rows, a pitch-to-diameter ratio of 6, and the 30°, 60° and 90° holes, respectively. The spanwise variation in effectiveness was reduced for all angles, and the value was similar to that in the two-inline rows of the same pitch and injection angle.

5. Summary and concluding remarks

Fig. 22 summarises the performance of all the configurations tested, in terms of laterally averaged effectiveness. The two-inline rows with a pitch-to-diameter ratio of 3, gave the largest effectiveness of 0.5 with 30° holes at x/D of 2.2. Lower maxima were achieved in descending order with the single row and a pitch-to-diameter ratio of 3 ($\overline{\eta}$ of 0.4), the two staggered rows with a pitch-to-diameter ratio of 6 ($\overline{\eta}$ of 0.32), the two-inline rows with a pitch-to-diameter ratio of 6 ($\overline{\eta}$ of 0.27), the single row with a pitch-to-diameter ratio of 6 ($\overline{\eta}$ of 0.23), and finally, the single hole ($\overline{\eta}$ of 0.22). This order was the same at all axial locations.

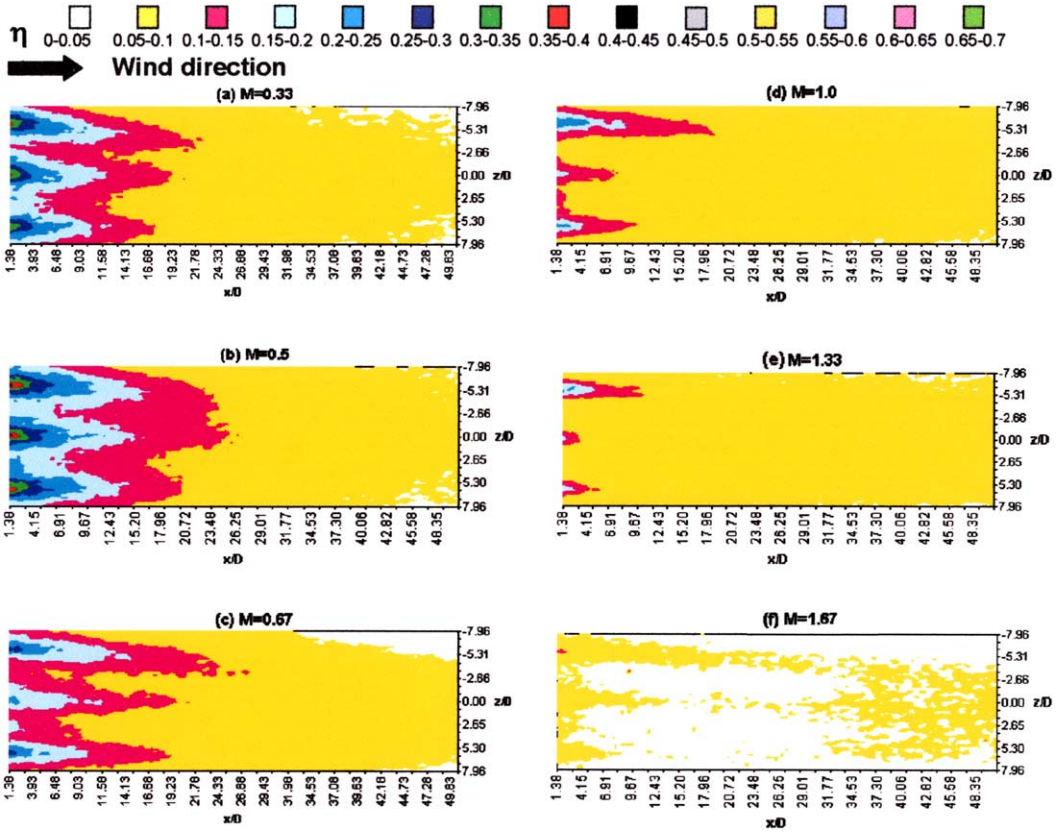

Fig. 20. Film cooling effectiveness for two staggered rows of 60° holes with p/D of 6 and s/D of 12.5 (only the centre 3 jets are shown).

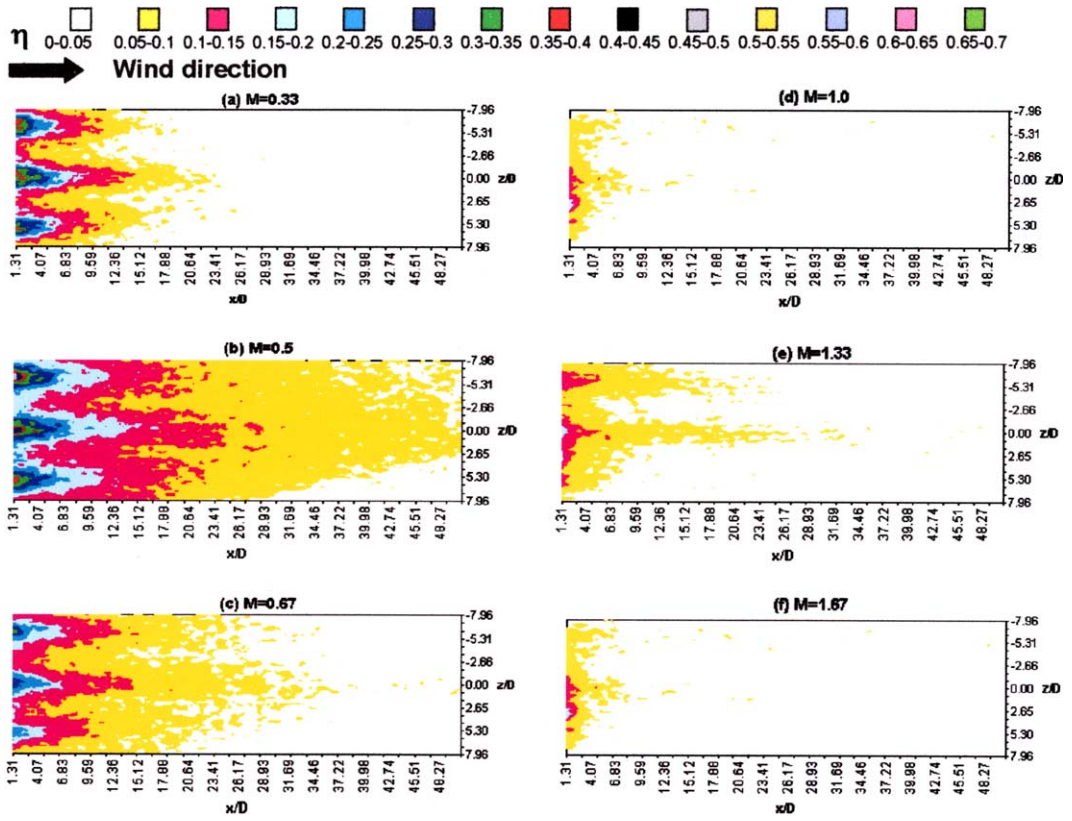

Fig. 21. Film cooling effectiveness for two staggered rows of 90° holes with p/D of 6 and s/D of 12.5 (only the centre 3 jets are shown).

The maximum $\overline{\eta}$ was achieved with a blowing ratio of 0.5 approximately at x/D equal to, or smaller than 5.2 for one row of 30° holes with pitch-to-diameter ratios of 3 and 6, which agreed with Goldstein et al. [32] and Liess [33]. And the blowing ratio at which the maximum effectiveness occurred increased with streamwise distance, since stronger jets travelled further downstream. This finding reinforces the need to specify the axial location when comparing the blowing ratio at which the maximum effectiveness occurred.

The maximum $\overline{\eta}$ with one row of 60° holes occurred with blowing ratios of less than 0.5 at x/D equal to, or smaller than 5.2 with pitch-to-diameter ratios of 3 and 6. The row of 90° holes gave lower values than the 30° and 60° holes due to greater vertical momentum and penetration. It is worth noting that the steeper the hole, the lower the blowing ratio at which the maximum effectiveness occurred in the near-hole region.

Fig. 22 also includes the results of other researchers. Ekkad et al. [34] found similar trends at x/D of 2.2 with the 30° holes. However, their measurements were some 50% lower than those reported here, probably due to the fact that their larger value of δ^*/D, twice that of 0.15 in the present experiments. Kohli and Bogard [35] and Pedersen et al. [8] had similar findings to those here, with the 30° and 60° holes at x/D of 5.2, and their value of δ^*/D were similar to that here. The differences between the current results and those of Brown and Saluja [10] and Pedersen et al. [8] at x/D of 13 were well within experimental uncertainty.

The spanwise uniformity and coverage in effectiveness were improved with the smaller pitch, particularly for the intermediate and far downstream regions. The variations of centreline effectiveness were similar for a row of 30° holes with pitch-to-diameters of 3 and 6, but the coverage was 75% greater with the smaller pitch-to-diameter ratio for blowing ratios below unity. For the row with 60° holes, the smaller pitch provided an average increase of 20% in the immediate region for blowing ratios below unity, and by 100% away from the holes ($x/D \geqslant 16$) for all blowing ratios, compared to the larger pitch-to-diameter ratio. For the row of 90° holes, the smaller pitch gave similar centreline values to the larger pitch in the vicinity of the holes, but increased the centreline values by 100% away from the holes. Thus, the smaller pitch-to-diameter ratio offers better protection over a large area of turbine blade for a given total mass flow.

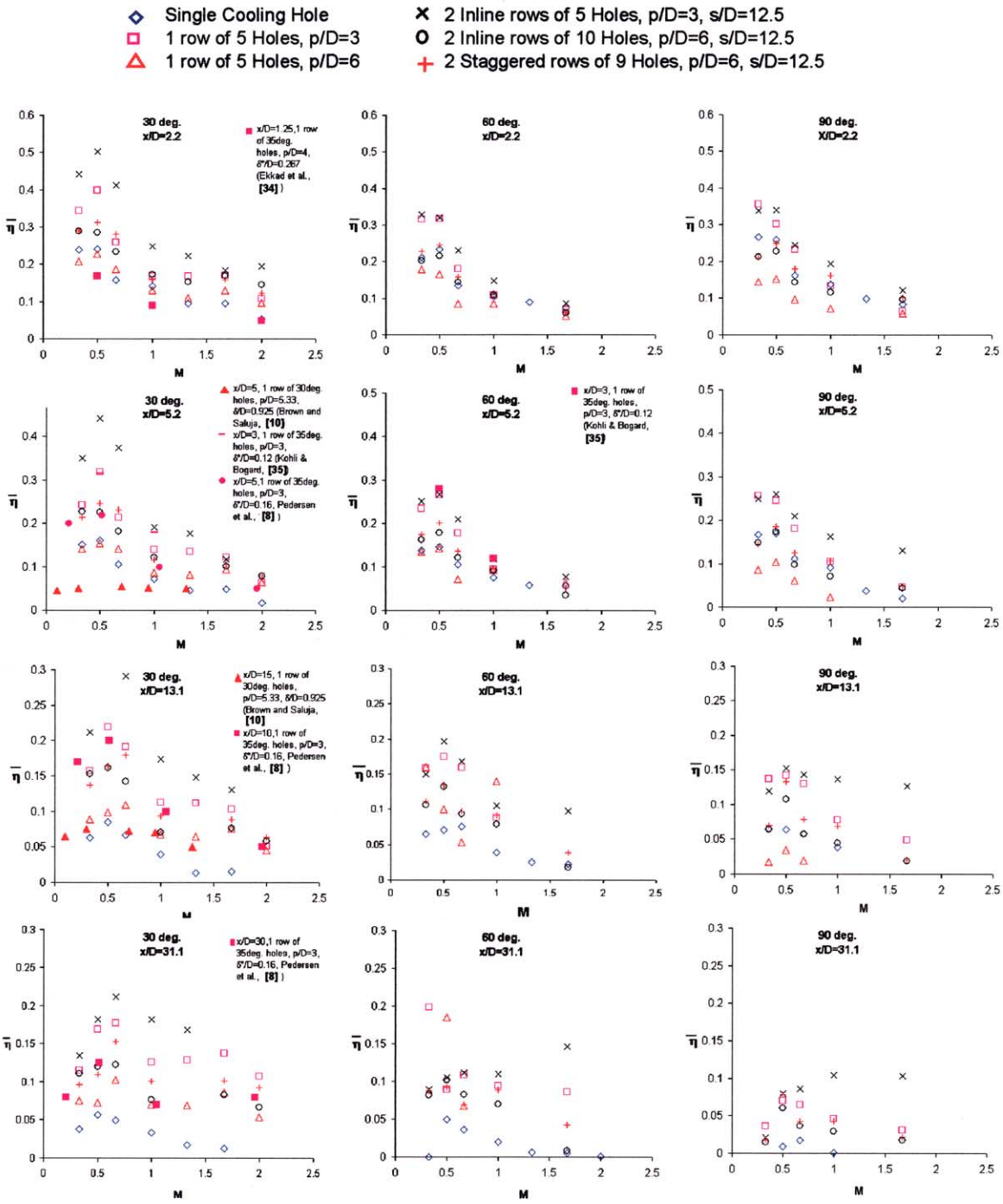

Fig. 22. Variations of laterally average effectiveness with blowing ratio for 30°, 60°, and 90° single holes, single rows and double rows.

The effectiveness and coverage with two-inline rows were generally better than one row even for the same injected mass flow. The benefits of the inline rows were greatest with the 30° holes, and became most apparent with blowing ratios greater than unity.

Acknowledgement

The authors would like to thank ABB Alstom Power Ltd., particularly Prof. J. Hannis, Dr. J. Turner, Dr. Gan for supporting the present work.

References

[1] C.H.N. Yuen, R.F. Martinez-Botas, Film cooling characteristics of a single hole at various streamwise angles: Part I. Effectiveness, Int. J. Heat Mass Transfer 46 (2003) 221–235.

[2] C.H.N. Yuen, R.F. Martinez-Botas, Film cooling characteristics of a single hole at various streamwise angles: Part II. Heat transfer coefficient, Int. J. Heat Mass Transfer 46 (2003) 237–249.

[3] C.H.N. Yuen, R.F. Martinez-Botas, Film cooling characteristics of rows of round holes at various streamwise angles: Part II. Heat transfer coefficient, Int. J. Heat Mass Transfer, in press, doi:10.1016/j.ijheatmasstransfer.2005.05.020.

[4] V.L. Eriksen, R.J. Goldstein, Heat transfer and film cooling following injection through inclined circular tubes, ASME J. Heat Transfer (May) (1974) 239–245.

[5] R.J. Goldstein, T. Yoshida, Boundary layer and laminar injection on film cooling performance, ASME J. Heat Transfer 104 (1982) 355–362.

[6] R.J. Goldstein, P. Jin, R.L. Olson, Film cooling effectiveness and mass/heat transfer coefficient downstream of one row of discrete holes, ASME Paper No. 98-GT-174, 1998.

[7] M.Y. Jabbari, R.J. Goldstein, Adiabatic wall temperature and heat transfer downstream of injection through two rows of holes, ASME J. Eng. Power 100 (1978) 303–307.

[8] D.R. Pedersen, E.R.G. Eckert, R.J. Goldstein, Film cooling with large density difference between the mainstream and the secondary fluid measured by the heat-mass transfer analogy, ASME J. Heat Transfer 99 (1977) 620–627.

[9] G. Bergeles, Three-dimensional discrete hole cooling processes: an experimental and theoretical study, Ph.D. thesis, University of London, Imperial College of Science, Technology and Medicine, London, 1976.

[10] A. Brown, C.L. Saluja, Film cooling from a single hole and a row of holes of variable pitch to diameter ratio, Int. J. Heat Mass Transfer 22 (1979) 525–533.

[11] A.K. Sinha, D.G. Bogard, M.E. Crawford, Film-cooling effectiveness downstream of a single row of holes with variable density ratio, ASME J. Turbomach. 113 (1991) 442–449.

[12] J.C. Han, A.B. Mehendale, Flat-plate film cooling with steam injection through one row and two rows of inclined holes, ASME J. Turbomach. 108 (1986) 137–144.

[13] R.J. Vedula, D.E. Metzger, A method for the simultaneous determination of local effectiveness and heat transfer distributions in three-temperature convection situations, ASME Paper presented at the International Gas Turbine and Aeroengine Congress and Exposition, Orlando, FL, June 3–6, 1991.

[14] S.V. Ekkad, J.-C. Han, Flat plate film cooling effectiveness and heat transfer using a transient liquid crystal technique, Paper presented at the ASME/JSME Thermal Engineering Conference, vol. 3, 1995, pp. 445–452.

[15] J.R. Pietrzyk, D.G. Bogard, M.E. Crawford, Hydrodynamics measurements of jets in crossflow for gas turbine film cooling applications, ASME J. Turbomach. 111 (2) (1989) 139–145.

[16] A.K. Sinha, D.G. Bogard, M.E. Crawford, Gas turbine film cooling: flowfield due to a second row of holes, ASME J. Turbomach. 113 (1991) 450–456.

[17] B. Jubran, A. Brown, Film cooling from two rows of holes inclined in the streamwise and spanwise directions, ASME J. Eng. Gas Turb. Power 107 (1985) 84–91.

[18] R.J. Margason, Fifty years of jet in crossflow research, AGARD Meeting on Computational and Experimental Assessment of Jets in Crossflow, April 1993.

[19] C.H.N. Yuen, Measurement of local heat transfer coefficient and film cooling effectiveness ion film cooling geometries, Ph.D. thesis, University of London, Imperial College of Science, Technology and Medicine, London, 2000.

[20] G. Bergeles, A.D. Gosman, J. Launder, The near-field character of a jet discharged normal to a mainstream, ASME J. Heat Transfer 98 (1976) 373–378.

[21] D. Crabb, D.F.G. Durao, J.H. Whitelaw, A round jet normal to a crossflow, ASME J. Fluids Eng. 103 (1981) 142–153.

[22] J. Andreopoulos, W. Rodi, An experimental investigation of jets in crossflow, J. Fluid Mech. 138 (1984) 93–127.

[23] D.K. Walters, J.H. Leylek, A detailed analysis of film cooling physics: part I—streamwise injection with cylindrical holes, ASME J. Turbomach. 122 (2000) 102–112.

[24] J.R. Pietrzyk, D.G. Bogard, M.E. Crawford, Effects of density ratio on the hydrodynamcis of film cooling, Trans. ASME J. Turbomach. 112 (2) (1990) 437–443.

[25] S.J. Kline, F.A. McClintock, Describing uncertainties in single-sample experiments, Mech. Eng. (January) (1953) 3–8.

[26] P.J. Schneider, Conduction Heat Transfer, sixth ed., Addison-Wesley, Reading, MA, 1974, pp. 176–181.

[27] H.H. Cho, D.H. Rhee, B.G. Kim, Film cooling effectiveness and heat/mass transfer coefficient around a conical-shaped hole with a compound angle injection, ASME paper presented at the International Gas Turbine and Aeroengine Congress and Exhibition, Indianapolis, IN, June 7–10, 1999, ASME paper 99-GT-38.

[28] Y. Yu, C.-H. Yen, T.I.-P. Shih, M.K. Chyu, S. Gogineni, Film cooling effectiveness and heat transfer coefficient distributions around diffusion shaped holes, ASME paper presented at the International Gas Turbine and Aeroengine Congress and Exhibition, Indianapolis, IN, June 7–10, 1999, ASME paper 99-GT-34.

[29] S. Baldauf, A. Schulz, S. Wittig, High resolution measurements of local effectiveness by discrete hole film cooling, ASME Paper presented at the International Gas Turbine and Aeroengine Congress and Exhibition, Indianapolis, IN, June 7–10, 1999, ASME paper 99-GT-46.

[30] Z.A. Khan, J.H. Whitelaw, Mean velocity and concentration characteristics of rows of jets in a crossflow, Imperial College Report FS/79/16, 1979.

[31] N.W. Foster, D. Lampard, The flow and film cooling effectiveness following injection through a row of holes, ASME J. Eng. Power 102 (1980) 584.

[32] R.J. Goldstein, E.R.G. Eckert, J.W. Ramsey, Film cooling with injection through holes: adiabatic wall temperatures downstream of a circular hole, ASME J. Eng. Power (1968) 384–395.

[33] C. Liess, Experimental investigation of film cooling with ejection from a row of holes from the application to gas turbine blades, ASME J. Eng. Power (January) (1975) 21–27.
[34] S.V. Ekkad, D. Zapata, J.C. Han, Film effectiveness over a flat surface with air and CO_2 injection, through compound angle holes using transient liquid crystal image method, ASME J. Turbomach. 119 (1997) 587–593.
[35] A. Kohli, D.G. Bogard, Adiabatic effectiveness, thermal Fields, and velocity fields for film cooling with large angle injection, in: International Gas Turbine and Aeroengine Congress and Exposition, Houston, TX, June 5–8, 1995, ASME 95-GT-219.